

## Application of neural-network-assisted flux surface mapping to diagnostic observations of Wendelstein 7-X's island divertor

A. Knieps<sup>1</sup>, M. Brenzke<sup>1</sup>, D. Böckenhoff<sup>1</sup>, P. Drews<sup>1</sup>, M. Endler<sup>2</sup>, Y. Gao<sup>2</sup>, J. Geiger<sup>2</sup>,

A. Krämer-Flecken<sup>1</sup>, Y. Liang<sup>1</sup>, F. Reimold<sup>2</sup>, Y. Suzuki<sup>3</sup>, S. Wiesen<sup>1</sup> and the W7-X team

<sup>1</sup> *Forschungszentrum Jülich GmbH, Institut für Energie- und Klimaforschungs Plasmaphysik,*

*Partner of the Trilateral Euregio Cluster (TEC), 52425 Jülich, Germany*

<sup>2</sup> *Max-Planck-Institut für Plasmaphysik, 17491 Greifswald, Germany*

<sup>3</sup> *Hiroshima University, 739-8527 Higashi-Hiroshima, Japan*

Plasma diagnostics in fusion research devices often observe distinct locations in the target plasma. To gain a consistent picture and separate geometric effects from 3D transport phenomena, these observations are commonly mapped into a radial coordinate, often using surfaces reconstructed by VMEC. Such an approach, however, can not map out magnetic islands and other non-nested magnetic topologies, which severely hampers its extension onto the plasma edge. To analyze the edge-core relationship and define approximate profiles in the plasma edge, we would like to construct a general approach to magnetic surface mapping, which does not require these surfaces to form simple nested topologies.

### Flux surface mapping

A surface label that serves well as a diagnostic mapping can be defined as the shortest path length from the magnetic axis to our points of interest, with the special modification that we only count the perpendicular component of the path motion when calculating the length.

$$r_{\perp}(x) = \min_{\substack{\gamma \in C^{1,p}([0,1], \mathbb{R}^3) \\ \gamma(0) \in S_{\text{ax}}, \gamma(1) = x}} \int_0^1 \left| \vec{B} \times \frac{d\gamma}{d\tau}(\tau) \right| d\tau$$

This label definition ensures constant values along magnetic field lines and has monotonic behavior inside magnetic island structures (with the O-points being local maxima and the outside-facing separatrix as local minima along sightlines). Furthermore, in a perfectly circular Tokamak-like geometry, it corresponds exactly to the minor radius.

Such a mapping has a straightforward approximation approach through brute-force distance calculations of Poincaré maps and shortest path graph algorithms. However, such a mapping is expensive to compute. To compensate for the computational expense, we trained a neural network to approximate the mapping based on position, vacuum configuration information (coil currents), axis current, and plasma beta using precomputed bulk evaluations.

### **Diagnostics used for initial comparison**

For an initial comparison, we used three diagnostic measurements in a discharge (ID 20180814.43) from the second Wendelstein 7-X divertor campaign (OP1.2b). We included three diagnostics, the Thomson scattering system [1] (which has a few channels in the plasma edge, the Helium beam line ratio spectroscopy [2], and Langmuir probe measurements from the combined probe [3] on the Multi-Purpose-Manipulator [4]. As can be seen in figure 1, all of these diagnostics measure the outer part of the island, but miss the O-point.

### **Cross-diagnostic comparison**

When plotting the diagnostic observations by their flux surface label, the profiles are folded into a structure where matching surfaces are overlapped with each other. Properly reading the profiles is best illustrated by the manipulator measurements in blue. The manipulator plunge is initiated outside the island separatrix, at an  $r_{\perp}$  value beyond the range of the plot. From its initial starting point, the manipulator first crosses into the island at the outer island separatrix, where the profile is folded for the first time. From there, it proceeds towards the inner parts of the islands with increasing  $r_{\perp}$  until reaching its closest approach to the O-point indicated by a local maximum in  $r_{\perp}$  (right dashed line - purple). As it moves towards the core,  $r_{\perp}$  decreases again, eventually crossing the separatrix again and plunging into the core. While the two profile values at the separatrix position are measured at the same magnetic island surface, they represent the edge- and core-facing sides of this surface (and therefore the up- and downstream regions).

A first good indicator for the consistency of the mapping can be observed from the self-overlap of the individual profiles near their folding points. This shows that some of the apparent linear variation in the diagnostic observations is primarily related to the nonuniform intersection between the sight lines and the magnetic surfaces.

Assuming that the mapping reflects the magnetic geometry reasonably well, one can then also compare the up- and downstream profiles on identical flux surface labels (a first light physics observations). It appears that the temperature measurements of all 3 diagnostics agree well near the O-point (respectively the closest approach) and from there towards the plasma core (with some minor divergences of the MPM near the O-point).

However, the density measurements between the different diagnostics seem to disagree more substantially, with the He beam measurements showing higher densities than Thomson scattering and MPM, while also having a local peaking structure near the O-point not visible in the other two diagnostics. Further investigations into these differences are a topic for future research.

Figure 1: Lines of sight of the employed diagnostics, as well as profiles of measured electron temperatures and densities (orange and blue resp.), and the flux surface label along the lines of sight (in green)

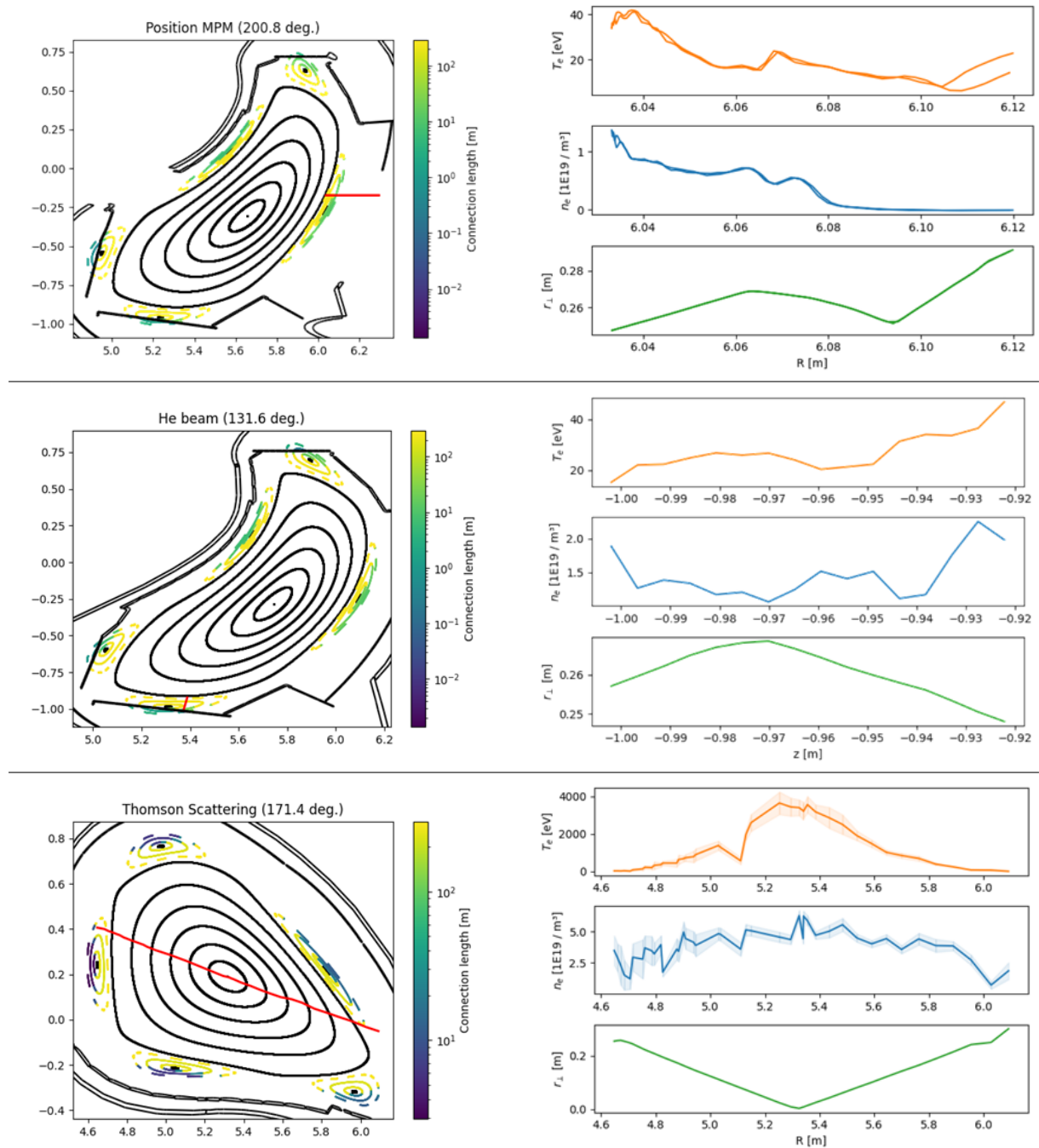
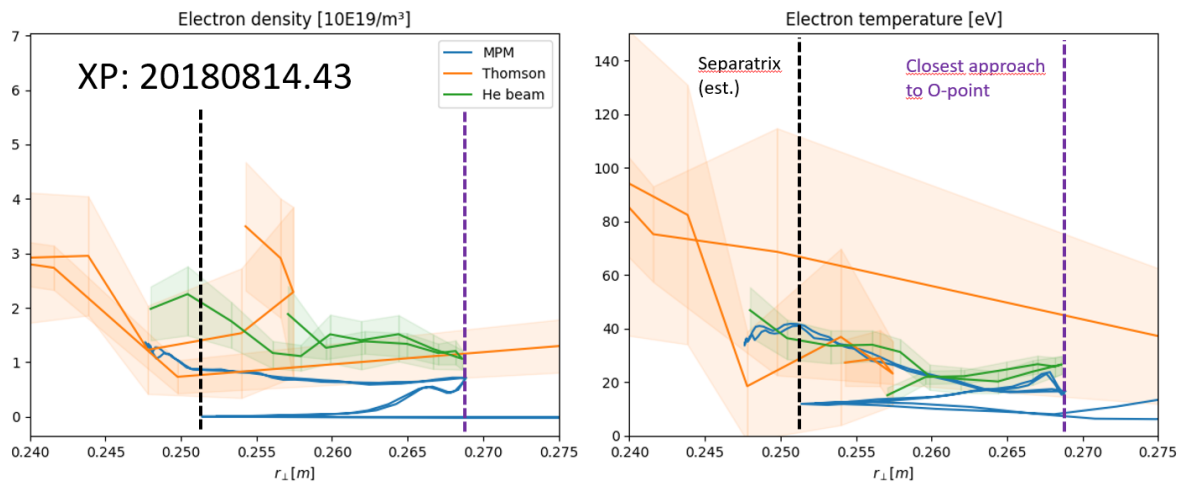


Figure 2: Cross-diagnostic comparison of electron temperature  $T_e$  and electron density  $n_e$  measurements from different diagnostics, mapped by their  $r_{\perp}$  flux surface label



## Acknowledgements

This work has been carried out within the framework of the EUROfusion Consortium, funded by the European Union via the Euratom Research and Training Programme (Grant Agreement No 101052200 — EUROfusion). Views and opinions expressed are however those of the author(s) only and do not necessarily reflect those of the European Union or the European Commission. Neither the European Union nor the European Commission can be held responsible for them.

The authors gratefully acknowledge the computing time granted by the John von Neumann Institute for Computing (NIC) and provided on the supercomputer JURECA [5] at Jülich Supercomputing Centre (JSC).

## References

- [1] S.A. Bozhkov et al, The Thomson scattering diagnostic at Wendelstein 7-X and its performance in the first operation phase, *Journal of Instrumentation* **12** (2017)
- [2] T. Barbui et al, The He/Ne beam diagnostic for line-ratio spectroscopy in the island divertor of Wendelstein 7-X, *Journal of Instrumentation* **17** (2019)
- [3] P. Drews et al, Measurement of the plasma edge profiles using the combined probe on W7-X, *Nuclear Fusion* **57** (2017)
- [4] C. Killer et al, Reciprocating probe measurements in the test divertor operation phase of Wendelstein 7-X, *Journal of Instrumentation* **17** (2022)
- [5] Jülich Supercomputing Centre, JURECA: Modular supercomputer at Jülich Supercomputing Centre, *Journal of large-scale research facilities* **A132**. A132 (2018)